

Syntheses, structures, and electroluminescence of new blue luminescent star-shaped compounds based on 1,3,5-triazine and 1,3,5-trisubstituted benzene

Jun Pang,^a Ye Tao,^a Stephan Freiberg,^a Xiao-Ping Yang,^a Marie D'Iorio^a and Suning Wang^{*a}

^aDepartment of Chemistry, Queen's University, Kingston, Ontario, K7L 3N6, Canada

^bInstitute for Microstructural Science, National Research Council, Ottawa, Canada K1A 0R6

Received 20th June 2001, Accepted 7th November 2001

First published as an Advance Article on the web 11th December 2001

Four novel blue luminescent star-shaped compounds 1,3,5-tris(di-2-pyridylamino)benzene, **1**, 1,3,5-tris[*p*-(di-2-pyridylamino)phenyl]benzene, **2**, 2,4,6-tris(di-2-pyridylamino)-1,3,5-triazine, **3**, and 2,4,6-tris[*p*-(di-2-pyridylamino)phenyl]-1,3,5-triazine, **4**, have been synthesized and fully characterized. Compounds **1**, **2** and **4** were prepared from the reactions of appropriate *s*-triazine and 1,3,5-trisubstituted benzene compounds with di-2-pyridylamine *via* copper-mediated Ullmann condensation in good yield (45–85%). Compounds **1**, **2** and **4** show glass formation. Compounds **1–4** emit a blue color both in solution and in the solid state. The emission maxima of compounds **1–4** in the solid state are at $\lambda = 412, 409, 393$ and 440 nm, respectively. Fluorescence quantum yields of compounds **1–4** are 0.53, 0.16, 0.43 and 0.78, respectively. Electroluminescent devices using compounds **1–4** as the emitters were fabricated.

Introduction

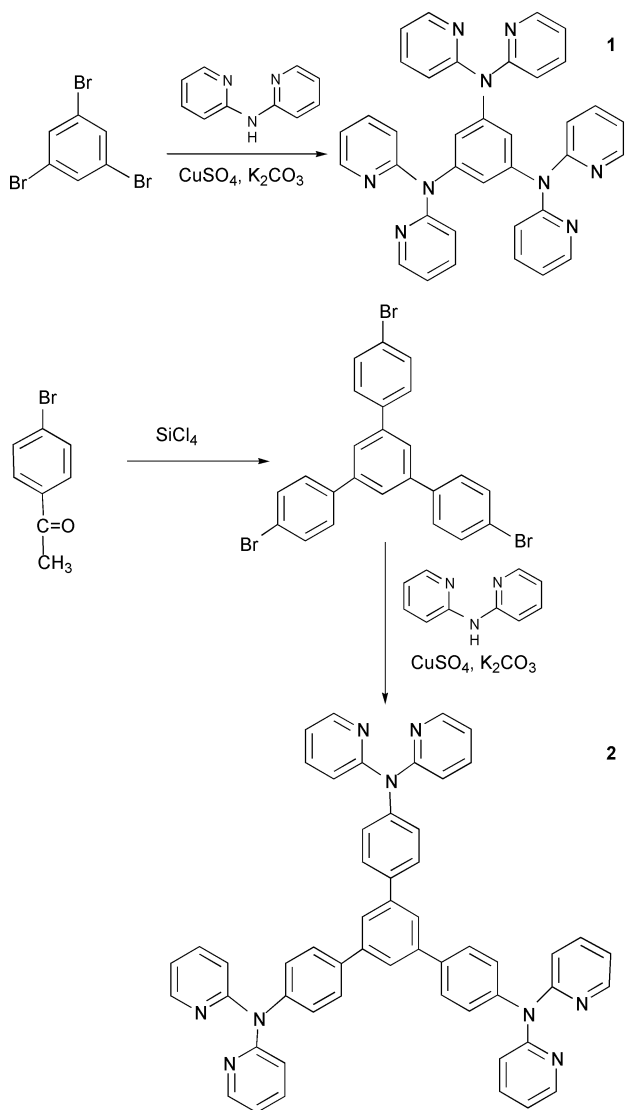
Organic-light-emitting-devices (OLEDs) have attracted a great deal of attention recently, due to their promising applications in electroluminescent displays.^{1,2} OLEDs are emerging as an attractive alternative display technology which has the potential to offer cheap materials, low power consumption, high brightness, and a wide viewing angle. To achieve full-color electroluminescent displays, three-color components, *i.e.*, blue, green and red must be available. Stable blue luminescent compounds that are useful in electroluminescent devices are still rare and very much in demand. We have demonstrated that di-2-pyridylamine or 7-azaindole can produce a bright blue luminescence when deprotonated and bound to either an aluminium ion or a boron center.³ However, many of our previously reported aluminium or boron compounds based on di-2-pyridylamine or 7-azaindole are not stable enough for electroluminescent devices. The instability of these compounds is mostly due to the fact that di-2-pyridylamine or 7-azaindole in the complexes is negatively charged. Our recent efforts have therefore focused on the attachment of the 7-azaindolyl or di-2-pyridylamino group to carbon atoms so that neutral and stable organic blue luminescent molecules can be achieved. Starburst or star-shaped organic molecules are an attractive class of molecules for OLEDs mostly because of their good film-forming properties.⁴ In fact some starburst organic molecules have been demonstrated recently by Shirota and other researchers to be effective emitters or hole or electron transport materials in OLEDs.^{1c,4} Therefore, we carried out the synthesis of a series of neutral π -conjugated star-shaped organic compounds based on di-2-pyridylamine and 7-azaindole. These new star-shaped molecules are analogues to several systems previously reported by Shirota and coworkers except that Shirota's molecules do not have the dipyridylamino or 7-azaindolyl functional groups. The dipyridylamino and 7-azaindolyl functional groups in the new star-shaped molecules can provide binding sites for metal ions, hence allowing the development of new luminescent star-shaped coordination compounds, which is the second motivation for this work. The star-shaped 7-azaindolyl compounds have been demonstrated

to be promising blue emitters in OLEDs and robust ligands for Pd(II) and Pt(II) complexes.^{5a–5c} The star-shaped di-2-pyridylamino derivatives based on 1,3,5-triazine and 1,3,5-trisubstituted benzene are effective chelate ligands for a variety of metal ions^{5d} and have the potential to function as blue emitters in OLEDs. Herein we report the details of syntheses, structures, and photoluminescent properties of four novel star-shaped molecules of di-2-pyridylamino derivatives based on 1,3,5-triazine and 1,3,5-trisubstituted benzene and the results of our preliminary investigation on their electroluminescent applications.

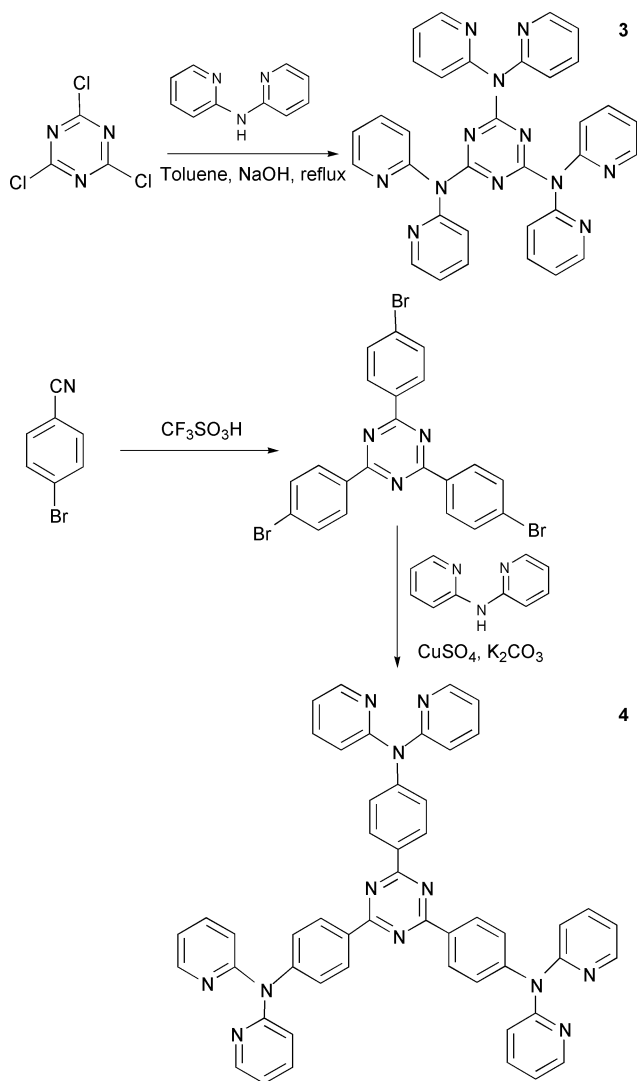
Results and discussion

Syntheses and characterization of compounds 1–4

The synthetic strategy employed for 1,3,5-tris(di-2-pyridylamino)benzene, **1**, 1,3,5-tris[*p*-(di-2-pyridylamino)phenyl]benzene, **2**, 2,4,6-tris(di-2-pyridylamino)-1,3,5-triazine, **3**, and 2,4,6-tris[*p*-(di-2-pyridylamino)phenyl]-1,3,5-triazine, **4** involved the preparation of star-shaped intermediates and their coupling to di-2-pyridylamine to form the final compounds. The classic technique for the construction of triarylamines has been the Ullmann condensation.^{6–10} In general, the reaction entails the condensation of an arylamine and an unactivated aryl halide with catalysis by some form of copper in the presence of a base. Compounds **1**, **2** and **4** were synthesized by using Ullmann condensation methods as shown in Schemes 1 and 2. The intermediates, 1,3,5-tris(*p*-bromophenyl)benzene and 2,4,6-tris(*p*-bromophenyl)-1,3,5-triazine for compounds **2** and **4** were synthesized by using modified literature methods.^{11,12} One key factor in Ullmann condensation reactions is the reaction temperature. If the temperature is not sufficiently high, no reaction or incomplete reaction occurs. On the other hand, too high a temperature results in extensive decomposition of starting materials and side reactions. Because some of our starting materials are still in the solid state at the reaction temperature, to ensure a relatively high yield of the reaction at a reasonable temperature, it is essential to pre-mix all starting materials well prior to the reaction to achieve maximum



Scheme 1



Scheme 2

contact area between reactants. Pre-mixing of all starting materials, base (K_2CO_3) and catalyst ($CuSO_4 \cdot 5H_2O$) was done using the procedures described in the Experimental section.

Steric hindrance also has an important effect on Ullmann condensation. With an increase in steric hindrance, the reaction becomes more difficult. The steric hindrance of the intermediates [1-(di-2-pyridylamino)-3,5-dibromobenzene and 1,3-bis(di-2-pyridylamino)-5-bromobenzene] involved in the synthesis of compound **1** is much higher than those involved in the syntheses of compounds **2** and **4**. Consequently the yields of compounds **2** and **4** are much higher than that of compound **1**. Compound **3** can be obtained readily by refluxing 2,4,6-trichlorotriazine with di-2-pyridylamine in toluene in the presence of NaOH. The yield of **3** is similar to that of **1**, attributable to the steric hindrance of intermediates involved in the reaction. In all syntheses, excess di-2-pyridylamine was used to maximize the yield of the trisubstituted product.

Compounds **1–4** were characterized by 1H and ^{13}C NMR and elemental analyses. For **1** and **3**, single crystals suitable for X-ray diffraction analyses were obtained and attempts to obtain suitable single crystals for X-ray diffraction analyses for **2** and **4** were unsuccessful. Independent confirmation of the molecular structures of **2** and **4** was achieved by the crystal structural determination of their metal coordination compounds.¹³ The crystal structures of **1** and **3** determined by X-ray diffraction analyses are shown in Fig. 1 and 2, respectively. The three amino nitrogen atoms in each structure

are co-planar with the central aromatic ring. The 2-pyridyl rings are not co-planar with the central ring due to steric interactions. A similar non-planar arrangement of 2-pyridyl groups has been observed in 4,4'-bis(di-2-pyridylamino) biphenyl and 1,4-bis(di-2-pyridylamino)benzene.¹⁴ The C–C and C–N bond lengths and angles observed in **1** and **3** are

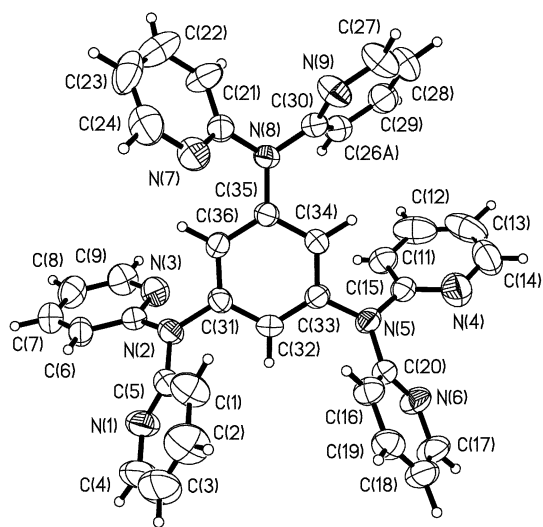


Fig. 1 A diagram showing the molecular structure of **1** with 50% thermal ellipsoids and labeling schemes.

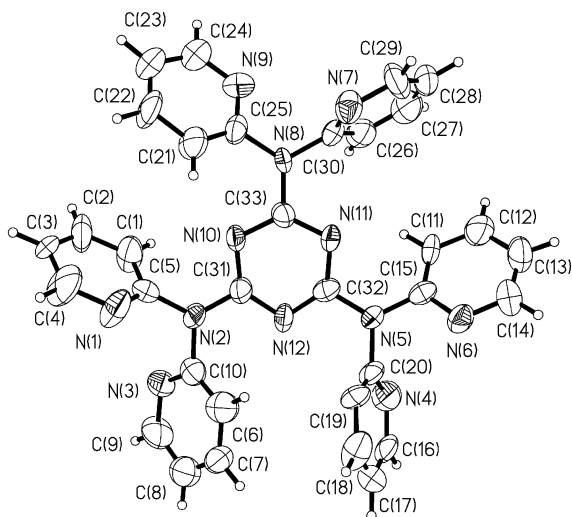


Fig. 2 A diagram showing the molecular structure of **3** with 50% thermal ellipsoids and labeling schemes.

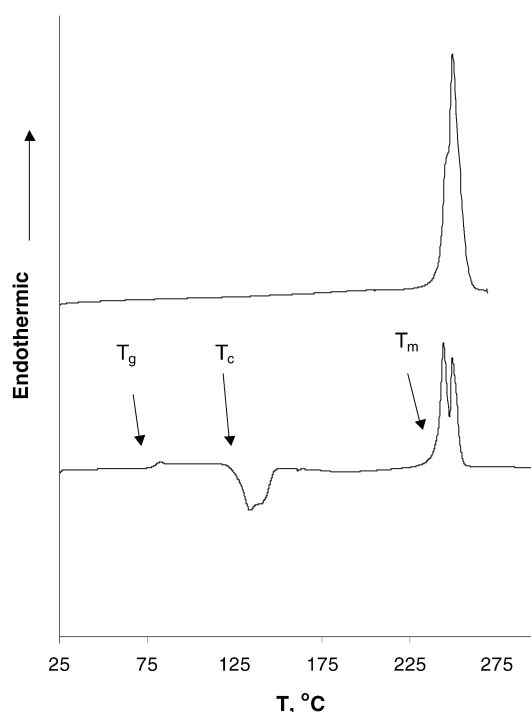


Fig. 3 DSC diagrams for **1**: top, first heating, $20\text{ }^{\circ}\text{C min}^{-1}$; bottom, second heating, $10\text{ }^{\circ}\text{C min}^{-1}$.

Table 1 Phase transition temperatures for **1–4**

Compound	$T_g/^{\circ}\text{C}$	$T_c/^{\circ}\text{C}$	$T_m/^{\circ}\text{C}$
1	80	126, 140	240, 248
2	128		187
3			299
4	121	180	267

Table 2 Luminescent and electronic properties of compounds **1–4**

Compound	Absorption λ/nm	PL (solid) $\lambda_{\text{max}}/\text{nm}$	PL (CH_2Cl_2) $\lambda_{\text{max}}/\text{nm}$	EL $\lambda_{\text{max}}/\text{nm}$	Quantum yield	HOMO/eV	LUMO/eV	Energy gap/eV
1	278, 322	412	415	404	0.53	-5.09	-1.64	3.45
2	323	409	385	410	0.16	-5.55	-2.13	3.42
3	320	393	433	396	0.43	-5.07	-1.35	3.72
4	322, 386	440	440	444	0.78	-4.99	-1.93	3.06

typical for aromatic molecules. There is intermolecular extensive π stacking in the crystal lattices of **1** and **3**. Although the molecular structures of **1** and **3** are very similar, the crystal lattices of these two molecules are not isomorphous as indicated by the unit cell parameters. Compounds **1** and **3** have also quite different melting points, $248\text{--}250\text{ }^{\circ}\text{C}$ versus $299\text{ }^{\circ}\text{C}$, which can be attributed to their packing difference in the crystal lattices. We have observed earlier that the replacement of a C–H in an aromatic group by one N atom in structurally closely related molecules indeed can result in a dramatic difference in crystal lattices and melting points.¹⁵ The most striking melting point difference was observed between compounds **2** ($187\text{ }^{\circ}\text{C}$) and **4** ($267\text{ }^{\circ}\text{C}$). TGA, DSC and elemental analyses indicated that the solid forms of **2** and **4** are likely to contain water molecules (\sim one water molecule per molecule of **2** or **4**), which may also play a role in the crystal lattice packing of **2** and **4**. All four compounds are thermally stable up to their melting points under air. The relatively high thermal stability of compounds **1–4** makes them possible candidates for applications in OLEDs.

The glass-forming properties and phase transition of compounds **1–4** were studied by DSC experiments. All four compounds were heated under argon with a heating rate of $20\text{ }^{\circ}\text{C per minute}$. Well-defined melting points were observed for all compounds. After first heating, all compounds were cooled to ambient temperature at a cooling rate of $20\text{ }^{\circ}\text{C per minute}$. The second heating with a rate of $10\text{ }^{\circ}\text{C per minute}$ was performed for all compounds. Compound **3** does not show glass formation, but compounds **1**, **2**, and **4** display well-defined glass transitions at $80\text{ }^{\circ}\text{C}$, $128\text{ }^{\circ}\text{C}$ and $121\text{ }^{\circ}\text{C}$, respectively. No crystallization was observed for compound **2** during the second heating while a broad crystallization peak starting at $\sim 180\text{ }^{\circ}\text{C}$ was observed for compound **4**. Most interestingly, compound **1** displays two overlapping crystallization peaks ($126\text{ }^{\circ}\text{C}$ and $140\text{ }^{\circ}\text{C}$) and two well resolved melting peaks at $240\text{ }^{\circ}\text{C}$ and $248\text{ }^{\circ}\text{C}$, respectively in the second heating (Fig. 3) (the melting peak of **1** was observed as a broad peak with a shoulder due to the faster scan rate) which are a clear indication that two crystal forms of **1** are present and they do not undergo interconversion before melting. Shirota's analogs of **1** and **3** [1,3,5-tris(diphenylamino)benzene and 1,3,5-tris(diphenylamino) triazine] do not show glass formation.^{4g} The behavior of **3** is consistent with Shirota's compound, but the glass-forming property of **1** is in contrast to that of 1,3,5-tris(diphenylamino)benzene. The presence of two crystalline forms in **1** may be responsible for its glass formation. The phase transition temperature data for **1–4** are summarized in Table 1. The relatively high thermal stability of compounds **1–4** and their ability to form the glass phase (except **3**) make them possible candidates for applications in OLEDs.

Photoluminescence and electroluminescence of **1–4**

Compounds **1–4** emit a blue color when irradiated by UV in the solid state or in solution. The di-2-pyridylamino moiety in the molecule is believed to be responsible for the blue luminescence based on our previous studies.^{5,14,16} However, the conjugation of the di-2-pyridylamino unit with the central portion of the star-shaped structure of **1–4** clearly has an impact on the emission energy as shown by the significant variation of emission energy listed in Table 2. In addition, the

emission bands of di-2-pyridylamine in solution and the solid state are at 343 nm and 362 nm, respectively. The red-shift of emission energy of **1–4**, compared to that of di-2-pyridylamine, is believed to be due to the conjugation of the nitrogen atom of the di-2-pyridylamino unit with the central aromatic unit of the star-shaped molecules. A similar red-shift of emission energy has been observed in several previously reported di-2-pyridylamino derivatives.^{14,16} The emission bands of **1–4** are fairly broad (band width at half height \approx 100 nm) in solution and the solid state. The fluorescent efficiencies of **1–4** in solution were determined to be 0.53, 0.16, 0.43 and 0.78, respectively (using 9,10-diphenylanthracene as the reference), indicating that these molecules are fairly efficient blue emitters and could be used in OLEDs.

To aid the design of electroluminescent devices, we studied the electronic properties of **1–4**. The oxidation potentials of **1–4** were obtained by electrochemical measurements using ferrocene as the standard. The HOMO energy levels relative to the vacuum level were calculated by using the oxidation potential (after being converted to the potential relative to the standard hydrogen electrode potential, NHE) and the ferrocene HOMO energy level of -4.8 eV (relative to the vacuum level) as the standard.¹⁷ The HOMO energy levels thus obtained for **1–4** are listed in Table 2. The band gaps were obtained from the absorption spectra (absorption edge) of the compounds. The LUMO energy level was calculated from the values of band gap and HOMO energy.

To evaluate the potential of molecules **1–4** in OLEDs, we carried out the fabrication of electroluminescent devices using **1–4** as the emitting layer. In all the electroluminescent devices fabricated, ITO (indium–tin–oxide) glass was used as the anode and aluminium was used as the cathode. As shown in Table 2, the HOMO levels of all four compounds are either similar to or slightly below that of ITO (-5.1 eV). Thus, a hole transport layer may not be necessary for the electroluminescent device. In contrast, the LUMO levels of all four compounds are much above that of the aluminium cathode (-4.2 eV). Therefore, to facilitate the electron injection, an electron transport layer PBD [2-(biphenyl-4-yl)-5-(4-*tert*-butylphenyl)-1,3,4-oxadiazole] with a LUMO energy of -2.4 eV, that is, between those of **1–4** and the work function of the aluminium cathode, was included in the device. In addition, on the anode, copper phthalocyanine (CuPc) was used to facilitate hole injections¹⁸ while LiF was used in the cathode to facilitate electron injection (LiF functions as an effective electron injector by tunneling injection¹⁹).

Electroluminescent devices for compounds **1–4** were fabricated by using the same device structure, ITO(1200 Å)/CuPc (100 Å)/compound **1–4**(500 Å)/PBD(200 Å)/LiF(10 Å)/Al(1500 Å). Compounds **1–4** are vacuum-deposited as amorphous films. A blue color was observed from all EL devices. The EL maxima for the four compounds listed in Table 2 approximately match those of PL as shown by Fig. 4 and 5, thus confirming that the observed blue color in the EL devices is from our compounds. The turn-on voltages for the devices using **1–4** are approximately 10 V, 9 V, 15 V and 15 V, respectively. The turn-on voltages of the triazine compounds **3** and **4** are much higher than those of **1** and **2**, perhaps an indication that the electron/hole mobility of **3** and **4** is poor. Inclusion of a hole transport layer TPD [*N,N'*-diphenyl-*N,N'*-bis(3-methylphenyl)biphenyl-4,4'-diamine] between the CuPc and the emitter layer in the EL device using **4** did decrease the turn-on voltage to about 6 V. However, a second EL peak at $\lambda = 532$ nm also appeared, which is, in fact, the dominating peak in the EL spectrum of the modified device using **4**. Because none of the materials used in the device have a PL peak in the green region, the 532 nm emission must be caused by an exciplex, likely between the TPD and compound **4** layers. The device using **3** is not stable and produces very weak blue emission ($L_{\max} = 14.7$ cd m⁻²), which could be caused by its

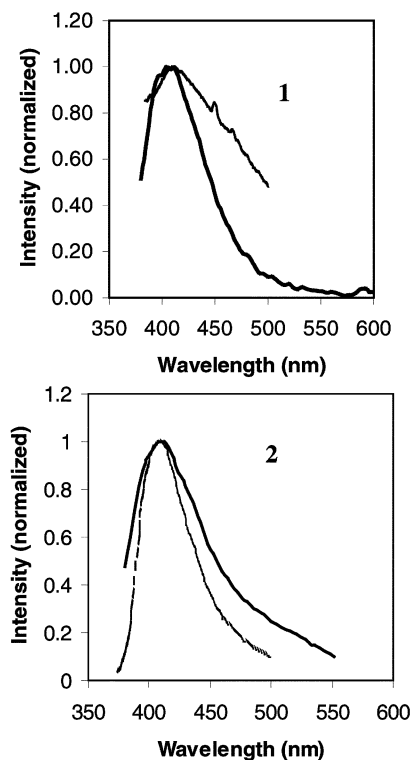


Fig. 4 PL (light line) and EL (heavy line) spectra of **1** (top) and **2** (bottom).

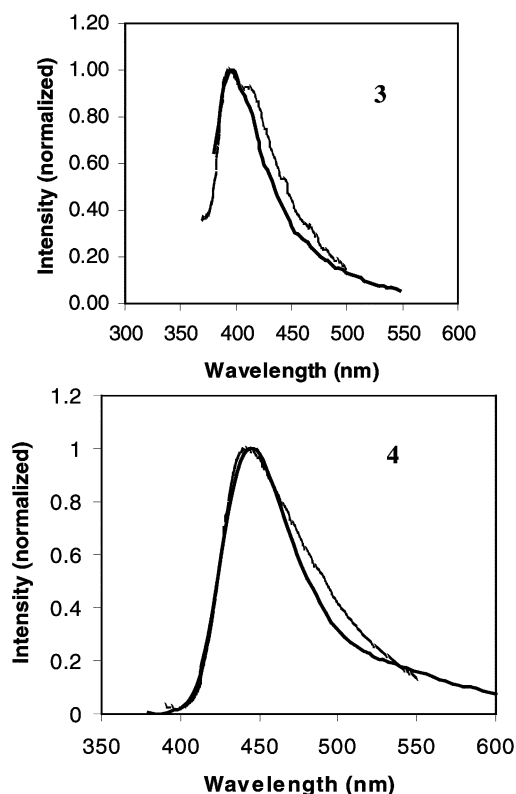


Fig. 5 PL (light line) and EL (heavy line) spectra of **3** (top) and **4** (bottom).

tendency to form crystals as evidenced by DSC measurements. The device using **1** is fairly stable but also produces weak blue emission ($L_{\max} = 19.2$ cd m⁻²). The best devices are from compounds **2** and **4**. The devices using **2** and **4** are much brighter than those using **1** and **3** as shown by the J - L - V diagrams in Fig. 6. Devices using compounds **1–4** as emitters

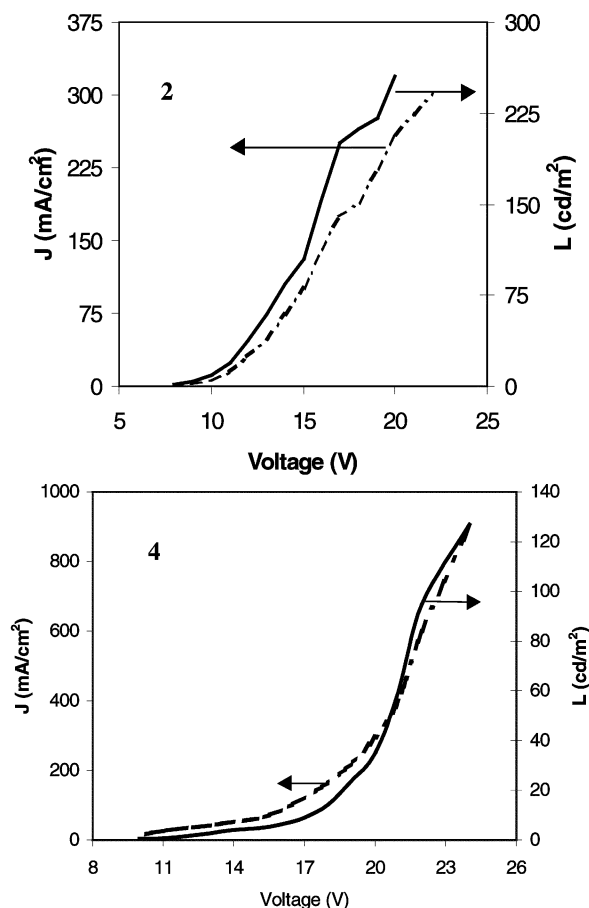


Fig. 6 J - L - V diagrams of **2** (top) and **4** (bottom).

and Alq_3 ($q = 8$ -hydroxyquinolinato) as the electron transport layer were also fabricated. However, instead of a blue color, only a green color from the Alq_3 layer was observed in these devices, indicating that Alq_3 is not a suitable electron transport material for compounds **1–4**.

The efficiencies of the present devices made from **2** and **4** are poor. Their performance could be improved by using other appropriate hole transport and electron transport materials to facilitate the charge transport of the devices. However, our current studies are limited by the availability of suitable hole/electron injecting materials. Nonetheless, the electroluminescent experiments established unambiguously that compounds **1–4** are promising blue emitters in electroluminescent devices and further study is necessary to optimize the performance of EL devices using compounds **1–4** as emitters. The fact that no hole transport materials are necessary for the EL devices of **1–4** suggests that these new compounds may also be able to function as hole transport materials in EL devices, which are being further investigated in our laboratory.

In summary, we have synthesized and characterized four novel star-shaped blue luminescent compounds based on di-2-pyridylamino derivatives of 1,3,5-triazine and 1,3,5-trisubstituted benzene. These four compounds are bright photoluminescent blue emitters, three of which have well-defined glass transition points. Although all four compounds are capable of functioning as blue emitters in electroluminescent devices, the two large star-shaped molecules **2** and **4** appear to be most promising.

Experimental section

All starting materials were purchased from Aldrich Chemical Company and used without further purification, unless otherwise stated. Tetrahydrofuran, hexane and toluene solvents were distilled from sodium and benzophenone under

a nitrogen atmosphere. Dichloromethane and chloroform were distilled from P_2O_5 under a nitrogen atmosphere. ^1H and ^{13}C NMR spectra were recorded on Bruker Advance 300 MHz spectrometers. Elemental analyses were performed by Canadian Microanalytical Service, Ltd, Delta, British Columbia. Excitation and emission spectra were recorded on a Photon Technologies International QuantaMaster Model C-60 spectrometer. Oxidation potentials were measured by using a CH_2Cl_2 solution on a CV-50 W Voltammetric Analyzer by using a Ag/AgCl electrode as the reference electrode and platinum electrode as the working electrode. Column chromatography was carried out on silica (silica gel 60, 70–230 mesh). Melting points were determined on a Fisher-Johns melting point apparatus. All DSCs were performed on a Perkin Elmer Pyris DSC 6. First heating and cooling scans were performed at 20 degrees per minute and the second heating scan was performed at 10 degrees per minute.

Synthesis of 1,3,5-tris(di-2-pyridylamino)benzene (1). A mixture of 1,3,5-tribromobenzene (0.94 g, 3.0 mmol) in dichloromethane (50 mL), di-2-pyridylamine (2.57 g, 15.0 mmol) in dichloromethane (50 mL), potassium carbonate (2.07 g, 15.0 mmol) in water (10 mL), copper sulfate (0.12 g, 0.492 mmol) in water (10 mL) was stirred and mixed well, and then evaporated to dryness under vacuum. After drying, the mixture was ground carefully in a mortar. To this mixture, 3–5 drops of dichloromethane were added. The mixture was heated at 210 °C for 8 h under N_2 . After being cooled to room temperature the mixture was dissolved in dichloromethane (100 mL) and water (100 mL). The organic layer was washed with water (3×100 mL), dried over Na_2SO_4 , and concentrated to give a yellow residue which was purified by a chromatographic column using THF–hexane (3 : 1) as the eluent to obtain a brown solid. Recrystallization from CH_2Cl_2 –hexane yielded colorless crystalline compound **1** (0.79 g, yield 45%). Mp 250 °C. ^1H NMR in CDCl_3 (δ , ppm, 298K): 8.28 (6H, d, $^3J = 4.8$ Hz, py), 7.56 (6H, dd, $^3J_1 = 8.4$, $^3J_2 = 7.2$ Hz, py), 7.14 (6H, d, $^3J = 8.4$ Hz, py), 6.91 (6H, dd, $^3J_1 = 7.2$, $^3J_2 = 4.8$ Hz, py), 6.78 (3H, s, ph). ^{13}C NMR in CDCl_3 (δ , ppm, 298 K): 158.0, 148.7, 146.8, 137.9, 120.6, 118.9, 117.9. Anal. Calcd for $\text{C}_{36}\text{H}_{27}\text{N}_9$: C, 73.83; H, 4.65; N, 21.52. Found: C, 73.01; H, 4.71; N, 21.58%.

Synthesis of 1,3,5-tris(*p*-bromophenyl)benzene. To a vigorously stirred solution of 4-bromoacetophenone (5.97 g, 30 mmol) in dry ethanol (60 mL) was added slowly silicon tetrachloride (10.2 g, 60 mmol) at 0 °C under N_2 . After stirring for 1 h at 0 °C, the mixture was warmed to room temperature, and then stirred for another 24 h. Water (100 mL) was added and the product was extracted with dichloromethane (3×100 mL). The organic layer was dried over Na_2SO_4 , and then concentrated under vacuum to give a yellow solid. Recrystallization from THF and hexane produced colorless needle crystals of the product (4.45 g, yield 82%). Mp 260–262 °C. ^1H NMR in CDCl_3 (δ , ppm, 298 K): 7.71 (3H, s), 7.63 (6H, d, $^3J = 6.6$ Hz), 7.56 (6H, d, $^3J = 6.6$ Hz).

Synthesis of 1,3,5-tris[*p*-(di-2-pyridylamino)phenyl]benzene (2). A mixture of 1,3,5-tris(*p*-bromophenyl)benzene (0.98 g, 1.8 mmol) in 50 mL of dichloromethane, di-2-pyridylamine (1.54 g, 9.0 mmol) in 50 mL of dichloromethane, potassium carbonate (1.24 g, 9.0 mmol) in 10 mL of water, copper sulfate (0.13 g, 0.518 mmol) in 10 mL of water was stirred and mixed well, and evaporated to dryness under vacuum. After drying, the mixture was ground carefully in a mortar. To this mixture, 3–5 drops of dichloromethane were added. The mixture was heated at 210 °C for 8 h under N_2 . After being cooled to ambient temperature, the mixture was dissolved in dichloromethane (100 mL) and water (100 mL). The organic layer was washed with water (3×100 mL), and then dried over Na_2SO_4 .

The organic layer was concentrated to give a yellow residue which was purified by a chromatographic column using THF–hexane (3 : 1) as the eluent to obtain **2** as a colorless crystalline solid (1.24 g, yield 85%). Mp 187 °C. ¹H NMR in CDCl₃ (δ, ppm, 298 K): 8.42 (6H, br d, ³J = 5.1 Hz, py), 7.79 (3H, s, ph1), 7.71 (6H, d, ³J = 8.6 Hz, ph2), 7.63 (6H, dd, ³J₁ = 8.6 Hz, ³J₂ = 6.9 Hz, py), 7.32 (6H, d, ³J = 8.6 Hz, ph2), 7.08 (6H, d, ³J = 8.6 Hz, py), 7.00 (6H, dd, ³J₁ = 6.9 Hz, ³J₂ = 5.1 Hz, py). ¹³C NMR in CDCl₃ (δ, ppm, 298 K): 158.0, 148.7, 144.5, 141.7, 138.1, 128.6, 126.9, 118.4, 118.3, 117.8, 117.5. Anal. Calcd for C₅₄H₃₉N₉·H₂O: C, 77.97; H, 4.93; N, 15.16. Found: C, 78.51; H, 4.75; N, 14.64%.

Synthesis of 2,4,6-tris(di-2-pyridylamino)-1,3,5-triazine (**3**).

To a stirred solution of 2,4,6-trichloro-1,3,5-triazine (1.85 g, 10 mmol) in toluene (150 mL), was added di-2-pyridylamine (7.70 g, 45 mmol) in toluene (80 mL). After stirring 0.5 h at ambient temperature, sodium hydroxide (1.56 g, 39 mmol) was added slowly to the mixture. After refluxing for 24 h, the mixture was cooled to room temperature and water (100 mL) was added to give a colorless solid. Recrystallization from dichloromethane and hexane produced **3** as a colorless crystalline solid (3.2 g, 55%). Mp 299–300 °C. ¹H NMR in CDCl₃ (δ, ppm, 298 K): 8.35 (6H, d, ³J = 5.1 Hz, py), 7.51 (6H, dd, ³J₁ = 8.1, ³J₂ = 7.5 Hz, py), 7.42 (6H, d, ³J = 8.1 Hz, py), 7.03 (6H, dd, ³J₁ = 7.5, ³J₂ = 5.1 Hz, py). ¹³C NMR in CDCl₃ (δ, ppm, 298 K): 165.4, 154.9, 148.3, 136.9, 122.7, 120.6. Anal. Calcd for C₃₃H₂₄N₁₂: C, 67.34; H, 4.11; N, 28.55. Found: C, 67.25; H, 4.18; N, 28.63%.

Synthesis of 2,4,6-tris(*p*-bromophenyl)-1,3,5-triazine. To a vigorously stirred solution of trifluoromethanesulfonic acid (6.00 g, 40 mmol) was dropwise added 4-bromobenzonitrile (3.64 g, 20 mmol) in dry CHCl₃ (50 mL) over the course of 1 h at 0 °C under N₂. After stirring for a further 1 h at 0 °C, the mixture was stirred for 24 h at ambient temperature and was poured into water containing small amount of NH₄OH. The organic layer was washed twice with water (2 × 40 mL), and then dried over Na₂SO₄. The solvent was evaporated *in vacuo*. The residue was recrystallized with dichloromethane and hexane to give a colorless solid (2.95 g, yield 81%). Mp > 300 °C. ¹H NMR in CDCl₃ (δ, ppm, 298K): 8.63 (6H, d, ³J = 8.7 Hz), 7.73 (6H, d, ³J = 8.7 Hz).

Synthesis of 2,4,6-tris[*p*-(di-2-pyridylamino)phenyl]-1,3,5-triazine (4**).** A mixture of 2,4,6-tris(*p*-bromophenyl)-1,3,5-triazine (1.32 g, 2.4 mmol) in dichloromethane (50 mL), di-2-pyridylamine (2.05 g, 12 mmol) in dichloromethane (50 mL), potassium carbonate (1.66 g, 12 mmol) in water (10 mL), copper sulfate (0.171 g, 0.686 mmol) in water (10 mL) was stirred and evaporated under vacuum. After drying, the mixture was ground carefully in a mortar. To this mixture, 3–5 drops of dichloromethane were added. The mixture was heated at 210 °C for 8 h under N₂. After the completion of the reaction, the mixture was cooled to room temperature and dissolved in dichloromethane (100 mL) and water (100 mL). The organic layer was washed with water (3 × 100 mL), and then dried over Na₂SO₄. The organic layer was concentrated to give a yellow residue which was purified by a chromatographic column using THF–hexane (3 : 1) as the eluant to obtain a yellow solid (1.18 g, yield 60%). Recrystallization from dichloromethane and hexane yielded colorless crystals of **4**. Mp 267–270 °C. ¹H NMR in CDCl₃ (δ, ppm, 298 K): 8.72 (6H, d, ³J = 8.7 Hz, ph), 8.41 (6H, d, ³J = 5.1 Hz, py), 7.64 (6H, dd, ³J₁ = 8.4, ³J₂ = 8.1 Hz, py), 7.32 (6H, d, ³J = 8.7 Hz, ph), 7.11 (6H, d, ³J = 8.1 Hz, py), 7.02 (6H, dd, ³J₁ = 8.4, ³J₂ = 5.1 Hz, py). ¹³C NMR in CDCl₃ (δ, ppm, 298 K): 171.1, 158.2, 149.3, 148.2, 138.1, 132.9, 130.8, 130.5, 125.5, 118.5. Anal. Calcd for C₅₁H₃₆N₁₂·H₂O: C, 73.38; H, 4.55; N, 20.14. Found: C, 73.88; H, 4.49; N, 20.28%.

Table 3 Crystallographic data

	1	3
Formula	C ₃₆ H ₂₇ N ₉	C ₃₃ H ₂₄ N ₁₂
FW	585.66	588.64
Space group	<i>P</i> 2 ₁ / <i>c</i>	<i>P</i> 2 ₁ / <i>c</i>
<i>a</i> /Å	12.675(3)	12.890(4)
<i>b</i> /Å	11.170(2)	19.438(6)
<i>c</i> /Å	20.954(4)	12.707(4)
β /deg	99.638(3)	116.380(6)
<i>V</i> /Å ³	2924.7(10)	2852.3(15)
<i>Z</i>	4	4
μ /cm ⁻¹	0.83	0.88
2 θ _{Max} /°	56.7	56.8
Reflns measured	20846	20657
Independent reflns	6976 (<i>R</i> _{int} = 0.06)	6762 (<i>R</i> _{int} = 0.24)
Parameters	514	406
Final <i>R</i> (<i>I</i> > 2 σ (<i>I</i>))	<i>R</i> ₁ ^a = 0.0426, <i>wR</i> ₂ ^b = 0.0693	<i>R</i> ₁ ^a = 0.0723, <i>wR</i> ₂ ^b = 0.1211
Goodness of fit on <i>F</i> ²	0.772	0.644
^a <i>R</i> ₁ = $\sum F_o - F_c /\sum F_o $. ^b <i>wR</i> ₂ = $[\sum w(F_o^2 - F_c^2)^2]/\sum[w(F_o^2)^2]^{1/2}$. <i>w</i> = $1/[\sigma^2(F_o^2) + (0.075P)^2]$, where <i>P</i> = $[\text{Max}(F_o^2, 0) + 2F_c^2]/3$.		

X-Ray crystallographic analyses†

Crystals of **1** and **3** were obtained from solutions of CH₂Cl₂–hexanes and were mounted on glass fibers. Data were collected on a Siemens Smart CCD 1000 diffractometer with graphite-monochromated Mo-K α radiation, operating at 50 kV and 35 mA at 23 °C, over a 2 θ range of 3–57°, respectively. Three standard reflections were measured every 197 reflections. No significant decay was observed for all samples during the data collection. Data were processed on a Pentium III PC using the Bruker AXS SHELXTL NT software package. Neutral atom scattering factors were taken from Cromer and Waber.²⁰ Both crystals belong to the monoclinic space group *P*2₁/*c*. All structures were solved by direct methods. All non-hydrogen atoms were refined anisotropically. The positions for all hydrogen atoms were either calculated or located directly from difference Fourier maps and their contributions in structural factor calculation were included. The crystallographic data are given in Table 3. Selected bond lengths and angles are given in Table 4.

Fabrication of electroluminescent devices

The EL devices using compounds **1–4** as the emitting layer were fabricated on an indium–tin-oxide (ITO) substrate, which was cleaned by an ultraviolet ozone cleaner immediately before use. Organic layers and a metal cathode composed of Al were deposited on the substrate by conventional vapor vacuum deposition. Prior to the deposition, all the organic materials were purified *via* a train sublimation method.²¹ A typical device structure used for all compounds is ITO(1200 Å)/CuPc (100 Å)/compound **1–4** (500 Å)/PBD (200 Å)/LiF (10 Å)/Al (1500 Å). No standard hole transport material was used. 2-(Biphenyl-4-yl)-5-(4-*tert*-butylphenyl)-1,3,4-oxadiazole (PBD) was employed as the electron transport layer in all devices. On the anode, copper phthalocyanine (CuPc) was used to facilitate hole injection while LiF was used in the cathode to facilitate electron injection. The active device area is 1.0 × 5.0 mm². The current–voltage characteristics were measured using a Keithley 238 current–voltage unit. The EL spectra and the luminance for the devices were measured by using a Photo Research-650 Spectra Colorimeter.

†CCDC reference numbers 166363 and 166364. See <http://www.rsc.org/suppdata/jm/b1/b105422h/> for crystallographic files in .cif or other electronic format.

Table 4 Selected bond lengths [Å] and angles [°] for **1** and **3**

1			
N(1)–C(4)	1.342(3)	N(9)–C(30)	1.321(2)
N(2)–C(5)	1.409(2)	N(9)–C(27)	1.341(3)
N(2)–C(10)	1.417(2)		
N(2)–C(31)	1.429(2)	C(5)–N(1)–C(4)	117.4(2)
N(3)–C(10)	1.335(2)	C(5)–N(2)–C(10)	121.38(17)
N(3)–C(9)	1.365(3)	C(5)–N(2)–C(31)	117.72(16)
N(4)–C(15)	1.348(2)	C(10)–N(2)–C(31)	119.37(16)
N(4)–C(14)	1.379(3)	C(10)–N(3)–C(9)	117.2(2)
N(5)–C(15)	1.409(2)	C(15)–N(4)–C(14)	115.3(2)
N(5)–C(20)	1.412(2)	C(15)–N(5)–C(20)	121.30(15)
N(5)–C(33)	1.430(2)	C(15)–N(5)–C(33)	117.73(15)
N(6)–C(20)	1.335(2)	C(20)–N(5)–C(33)	120.42(16)
N(6)–C(17)	1.338(2)	C(20)–N(6)–C(17)	115.83(19)
N(7)–C(25)	1.336(2)	C(25)–N(7)–C(24)	116.3(2)
N(7)–C(24)	1.344(3)	C(35)–N(8)–C(30)	120.46(16)
N(8)–C(35)	1.409(2)	C(35)–N(8)–C(25)	121.74(16)
N(8)–C(30)	1.416(2)	C(30)–N(8)–C(25)	117.45(16)
N(8)–C(25)	1.416(2)	C(30)–N(9)–C(27)	116.5(2)
3			
N(1)–C(5)	1.309(8)	N(11)–C(33)	1.351(7)
N(1)–C(4)	1.387(8)	N(11)–C(32)	1.353(6)
N(2)–C(31)	1.370(6)	N(12)–C(31)	1.320(6)
N(2)–C(5)	1.409(8)	N(12)–C(32)	1.325(7)
N(2)–C(10)	1.458(7)		
N(3)–C(10)	1.325(7)	C(5)–N(1)–C(4)	117.7(8)
N(3)–C(9)	1.340(6)	C(31)–N(2)–C(5)	122.8(6)
N(4)–C(16)	1.377(7)	C(31)–N(2)–C(10)	120.6(6)
N(4)–C(20)	1.390(7)	C(5)–N(2)–C(10)	116.5(6)
N(5)–C(32)	1.377(7)	C(10)–N(3)–C(9)	116.8(7)
N(5)–C(15)	1.432(7)	C(16)–N(4)–C(20)	113.7(7)
N(5)–C(20)	1.434(7)	C(32)–N(5)–C(15)	123.4(6)
N(6)–C(14)	1.331(7)	C(32)–N(5)–C(20)	119.0(6)
N(6)–C(15)	1.338(7)	C(15)–N(5)–C(20)	117.0(6)
N(7)–C(30)	1.348(7)	C(14)–N(6)–C(15)	115.6(7)
N(7)–C(29)	1.351(7)	C(30)–N(7)–C(29)	114.2(7)
N(8)–C(33)	1.390(6)	C(33)–N(8)–C(25)	123.3(6)
N(8)–C(25)	1.429(7)	C(33)–N(8)–C(30)	118.3(6)
N(8)–C(30)	1.442(7)	C(25)–N(8)–C(30)	118.4(5)
N(9)–C(24)	1.330(8)	C(24)–N(9)–C(25)	114.1(7)
N(9)–C(25)	1.337(8)	C(33)–N(10)–C(31)	110.7(6)
N(10)–C(33)	1.352(7)	C(33)–N(11)–C(32)	111.1(6)
N(10)–C(31)	1.354(6)	C(31)–N(12)–C(32)	112.9(6)

Acknowledgement

We thank the Natural Sciences and Engineering Research Council of Canada and the Xerox Research Foundation for financial support. We thank Dr Almeria Natansohn for providing access to the DSC instrument.

References

- (a) C. W. Tang and S. A. VanSlyke, *Appl. Phys. Lett.*, 1987, **51**, 913; (b) C. W. Tang, S. A. VanSlyke and C. H. Chen, *J. Appl. Phys.*, 1989, **65**, 3611; (c) Y. Shirota, Y. Kuwabara, H. Inada, T. Wakimoto, H. Nakada, Y. Yonemoto, S. Kawami and K. Imai, *Appl. Phys. Lett.*, 1994, **65**, 807; (d) Y. Hamada, T. Sano, M. Fujita, T. Fujii, Y. Nishio and K. Shibata, *Jpn. J. Appl. Phys.*, 1993, **32**, L514; (e) V. Bulovic, G. Gu, P. E. Burrows and S. R. Forrest, *Nature*, 1996, **380**, 29.
- (a) N. X. Hu, M. Esteghamatian, S. Xie, Z. Popovic, B. Ong, A. M. Hor and S. Wang, *Adv. Mater.*, 1999, **11**, 1460; (b) C. Adachi, T. Tsutsui and S. Saito, *Appl. Phys. Lett.*, 1990, **56**, 799; (c) X. T. Tao, H. Suzuki, T. Wada, H. Sasabe and S. Miyata, *Appl. Phys. Lett.*, 1999, **75**, 1655; (d) Z. Shen, P. E. Burrows, V. Bulovic, S. R. Forrest and M. E. Thompson, *Science*, 1997, **276**, 2009; (e) H. Aziz, Z. Popovic, N. X. Hu, A. M. Hor and G. Xu, *Science*, 1999, **283**, 1900; (f) Y. Hamada, T. Sano, H. Fujii, Y. Nishio, H. Takahashi and K. Shibata, *Appl. Phys. Lett.*, 1997, **71**, 3338; (g) C. H. Chen and J. Shi, *Coord. Chem. Rev.*, 1998, **171**, 161.
- (a) S. Wang, *Coord. Chem. Rev.*, 2001, **215**, 79; (b) J. Ashenhurst, L. Brancalion, A. Hassan, W. Liu, H. Schmider, S. Wang and Q. Wu, *Organometallics*, 1998, **17**, 3186; (c) J. Ashenhurst, G. Wu and S. Wang, *J. Am. Chem. Soc.*, 2000, **122**, 2541; (d) S. Gao, Q. Wu, G. Wu and S. Wang, *Organometallics*, 1998, **17**, 4666; (e) A. Hassan and S. Wang, *Commun. Chem.*, 1998, 211; (f) J. Ashenhurst, L. Brancalion, S. Gao, L. Wang, H. Schmider and S. Wang, *Organometallics*, 1998, **17**, 5334.
- (a) N. Tamoto, C. Adachi and K. Nagai, *Chem. Mater.*, 1997, **9**, 1077; (b) Z. Gao, C. S. Lee, L. Bello, S. T. Lee, R. M. Chen, T. Y. Luh, J. Shi and C. W. Tang, *Appl. Phys. Lett.*, 1999, **74**, 865; (c) Y. Shirota, K. Okumoto and H. Inada, *Synth. Met.*, 2000, **111**, 387; (d) S. Berleb, W. Brutting, M. Schwoerer, R. Wehrmann and A. Elschner, *J. Appl. Phys.*, 1998, **83**, 4403; (e) K. Itano, T. Tsuzuki, H. Ogawa, S. Appleyard, M. R. Willis and Y. Shirota, *IEEE Trans. Electron Devices*, 1997, **44**, 1218; (f) Y. Kuwabara, H. Ogawa, H. Inada, N. Noma and Y. Shirota, *Adv. Mater.*, 1994, **6**, 677; (g) I. Y. Wu, J. T. Lin, Y. T. Tao and E. Balasubramaniam, *Adv. Mater.*, 2000, **12**, 668; (h) E. Ueta, H. Nakano and Y. Shirota, *Chem. Lett.*, 1994, 2397; (i) Y. Shirota, *J. Mater. Chem.*, 2000, **10**, 25.
- (a) Q. Wu, A. Hook and S. Wang, *Angew. Chem., Int. Ed.*, 2000, **39**, 3933; (b) Q. Wu, Y. Tao, M. D'Iorio and S. Wang, *Chem. Mater.*, 2001, **13**, 71; (c) D. Song, Q. Wu, A. Hook and S. Wang, *Organometallics*, 2001, **20**, 4683; (d) J. Pang, E. J. P. Marcotte, C. Seward, S. Brown and S. Wang, *Angew. Chem., Int. Ed. Engl.*, 2001, **40**, 4042.
- K. D. Belfield, K. J. Schafer, W. Mourad and B. A. Reinhardt, *J. Org. Chem.*, 2000, **65**, 4475.
- H. B. Goodbrand and N. X. Hu, *J. Org. Chem.*, 1999, **64**, 670.
- A. J. Paine, *J. Am. Chem. Soc.*, 1987, **109**, 1496.
- P. E. Fanta, *Synthesis*, 1974, **1**, 9.
- J. Lindley, *Tetrahedron*, 1984, **40**, 1433.
- S. S. Elmersy, A. Pelter and K. Smith, *Tetrahedron Lett.*, 1991, **32**, 4175.
- S. Hayami and K. Inoue, *Chem. Lett.*, 1979, 545.
- J. Pang and S. Wang, unpublished results.
- W. Yang, L. Chen and S. Wang, *Inorg. Chem.*, 2001, **40**, 507.
- S. F. Liu, Q. Wu, H. L. Schmider, H. Aziz, N. X. Hu, Z. Popovic and S. Wang, *J. Am. Chem. Soc.*, 2000, **122**, 3671.
- W. Yang, H. Schmider, Q. Wu, Y. S. Zhang and S. Wang, *Inorg. Chem.*, 2000, **39**, 2397.
- J. Pommerehne, H. Vestweber, W. Guss, R. F. Mahrt, H. Bassler, M. Porsch and J. Daub, *Adv. Mater.*, 1995, **7**, 551.
- Y. Liu, H. Ma and A. K-Y. Jen, *Chem. Mater.*, 1999, **11**, 27.
- L. S. Hung, C. W. Tang and M. G. Mason, *Appl. Phys. Lett.*, 1997, **70**, 13.
- D. T. Cromer and J. T. Waber, *International Tables for X-ray Crystallography*, Kynoch Press, Birmingham, UK, 1974, Vol. 4, Table 2.2A.
- H. J. Wagner, R. O. Loutfy and C. K. Hsiao, *J. Mater. Sci.*, 1982, **17**, 2781.